Available online at www.eccomasproceedia.org
Eccomas Proceedia COMPDYN (2023) 2217-2228

ECCOMAS
Proceedia

COMPDYN 2023
9th ECCOMAS Thematic Conference on
Computational Methods in Structural Dynamics and Earthquake Engineering
M. Papadrakakis, M. Fragiadakis (eds.)
Athens, Greece, 12-14 June 2023

FULL-SCALE SHAKE TABLE TESTS OF A R.C. BUILDING EQUIPPED WITH AN ACTIVE MASS DAMPER: EXPERIMENTAL RESULTS AND NUMERICAL SIMULATIONS

G. Rebecchi[1], F. Menardo[1], M. Rosti[1], A. Bussini[1], P.M. Calvi[2]

[1] ISAAC s.r.l.
via dell'Agricoltura 1, Gaggiano (Milano), Italy
{giovanni.rebecchi, fabio.menardo, matteo.rosti, alberto.bussini}@isaacsrl.com

[2] Department of Civil and Environmental Engineering, University of Washington
Seattle, US
pmc85@uw.edu

Abstract

ISAAC antisismica is an Italian start-up based in Milan born in 2018 within the Mechanical Engineering Department of Politecnico di Milano. The company designs and produces active control systems for the seismic protection of existing and new buildings. The installation of these active systems involves a non-invasive process that does not impact architectural features and does not affect building functionality. In 2021 ISAAC developed and tested the first prototype of an Active Mass Damper (AMD), called I-Pro 1. The experimental program involved shake-table testing of two identical full-scale reinforced concrete frame buildings, but one equipped with the AMD. This paper presents the results of said experimental program and discusses the results of the numerical simulations performed as back analysis of the tests, by means a commercial FEM software. The research demonstrated that the proposed AMD is extremely effective at enhancing building seismic performance. Specifically, the AMD provided displacement reductions in the order of 70% and was shown capable of absorbing more than 60% of the total input energy. Thus, the un-retrofitted structure suffered nontrivial structural and non-structural damage, while the AMD-retrofitted building remained virtually undamaged at all shaking intensities considered. The numerical analyses demonstrate that accurate estimates of the response of AMD-equipped buildings can be achieved through relatively simple modeling, for example by simulating the active control system through a native dashpot link in any FEM commercial software.

Keywords: Active mass damper, full-scale shake table, reinforced-concrete buildings, enhancing seismic performance, back analysis, non-linear time history analysis.

ISSN:2623-3347
Peer-review under responsibility of the organizing committee of COMPDYN 2023.
doi: 10.7712/120123.10554.20294

1 INTRODUCTION

Active seismic response control systems can improve the dynamic performance of buildings and, at the same time, provide non-stop structural monitoring. The use of these systems is already addressed by international regulations (e.g., ISO 3010:2017), and identified as viable solutions that can be adopted to enhance the seismic response of new or existing buildings.

A novel servo-controlled Active Mass Damper (AMD) for the protection of structures against the effects of earthquakes was recently proposed in [1]. A prototype is shown in Figure 1. It consists of an innovative inertial system used as Active Vibration Control device that, differently from other AMDs, uses an electro-hydraulic actuator to move the inertial mass. The design, fabrication and preliminary testing of the AMD prototype has been carried out at the Politecnico di Milano, Italy. A brief description of the system is provided herein, taken from the companion paper [2]. For a more comprehensive discussion on active mass dampers, interested readers can refer to [3] - [12].

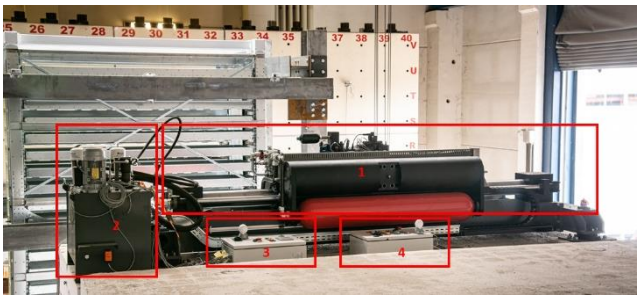

Figure 1: The AMD proposed: 1) hydraulic cylinder; 2) oil restoration control unit; 3) control panel and fault management; 4) control panel and fault management of hydraulic control unit.

The AMD prototype is made up of a fixed part which transmits the force to the floor of the building it is connected to, and a moving part which is responsible for generating the control force. The purpose of the AMD is to generate inertial forces that "counteract" the movement of the building by reducing the amplitude of oscillation and, consequently, the earthquake-induced forces experienced by the structural elements. The magnitude of the inertial forces to be generated is calculated in real time by the control algorithm, based on the accelerometric readings of sensors installed at certain locations across the structure.

The AMD comprises four main subsystems: sensors, controller, actuators and power system. The sensors are elements which provide the feedback needed for the control. They are installed on the structure to measure system response variables, such as displacements, velocities and accelerations. The sensors can also be used to perform tasks such as structural health monitoring, by allowing the dynamic identification of the structure during its life cycle.

The controller is the core of the AMD because it implements the vibrating control algorithm. It produces actuation signals by a feedback function of sensor measurements and defines the inertial mass displacement in time. The “Sky-Hook”, a direct velocity feedback control which does not need the creation of a building model, was chosen for its performance and robustness. The algorithm defines a control force ($F_{control}$) proportional to the relative velocity ($v_{relative}$) of the building through the constant G (gain) and this force is produced by the double acting hydraulic actuator used to move the inertial mass:

$$F_{control} = - G \cdot v_{relative} \tag{1}$$

The actuator can generate a linear force up to 220 kN, with maximum velocity and displacement amplitude of 5 m/s and ±0.5m, respectively.

This paper summarizes the key takeaways from the experimental program, pertaining to the performance of the proposed AMD, and presents the results of numerical simulations performed as back analysis, intended to identify an accurate yet simple way to model the AMD in a commercial FEM software.

2 BRIEF DESCRIPTION OF THE EXPERIMENTAL TESTS

2.1 Description of the setup

The assessment of the seismic performance of the proposed AMD was performed via shake-table testing of two nominally identical full-scale reinforced concrete frame structures with masonry infills, one of which equipped with the AMD, installed on the roof (see [1]).

The elevation views of the nominally identical full-scale specimens are shown in Figure 2a). The two specimens were 3-story one-bay (in both directions) frame buildings, made of RC columns with 20 x 20 cm cross section, connected to 40 cm thick RC slabs. The columns were reinforced with 4 longitudinal 16 mm diameter steel bars in the corners, and 8 mm diameter closed stirrups spaced at 100 mm (Figure 2b).

The floor plan dimensions were 5.0 x 2.1 m, and the clear inter-story height was 2.5 m. Infill masonry walls made of 8 x 25 x 25 cm clay blocks were installed in the N-S direction (i.e., the excitation direction) at each floor.

The two specimens were connected to the same foundation slab, which was bolted down to the shake table using post-tensioned steel bars.

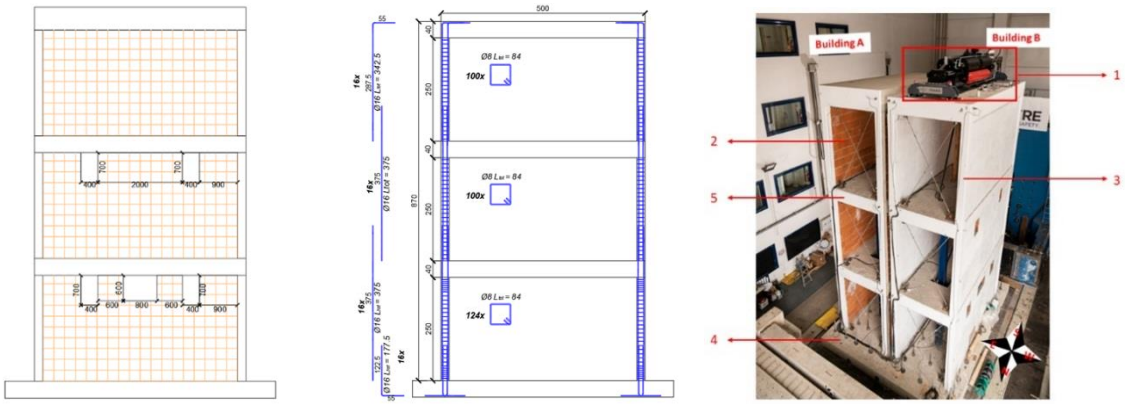

Figure 2: a) Elevation view of the buildings; b) Reinforcement details of the columns; (c) The buildings tested in the Eucentre laboratory: 1) AMD; 2) masonry infills; 3) columns; 4) foundation slab connected to the shake table; 5) floor slabs.

A view of the buildings and AMD control system in their pre-test configuration is shown in Figure 2c).

The response of both the shake table and the specimens was monitored in real time through an array of instruments including 20 accelerometers, 19 displacement transducers and an optical acquisition.

2.2 Tests protocol

The full-scale specimens were tested on the unidirectional shake table in the Shake-LAB at the Eucentre facility, Italy.

The specimens were tested by applying the E-W component of the Irpinia earthquake, which hit central Campania and central-northern Basilicata on the 23rd of November 1980. (PGA 0.32g).

The shake table experiments were conducted in 5 phases, over the course of three days. Each testing phase involved the application of the reference earthquake, considering scale factors ranging from 0.10 to 1.37, for a total of 19 tests, labelled CMP1 to CMP19. More details can be found in Rebecchi et al. (2022).

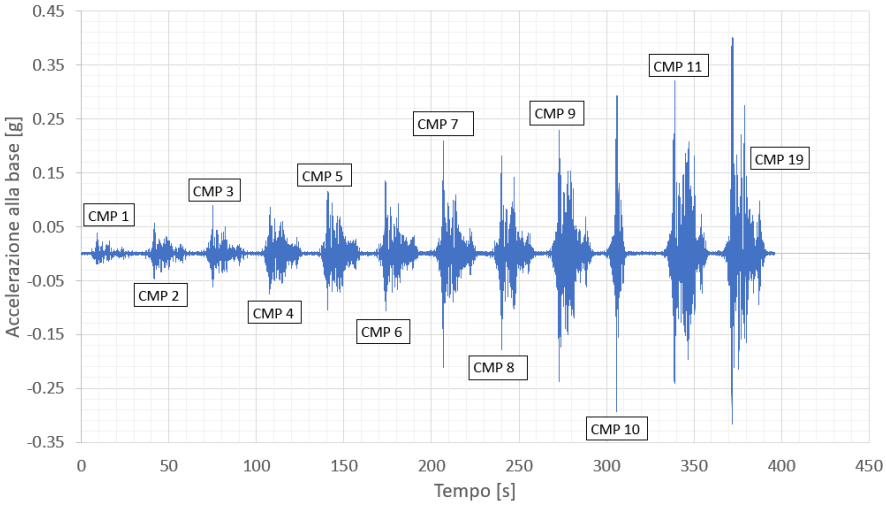

Figure 3 – Overall time history of the earthquake generated with the shaking table.

Furthermore, random wave tests were performed at the beginning of each testing phase in order to determine the progressive variation of the dynamic characteristics of the two buildings.

This technique was also used to identify the modal parameters of interest in order to appropriately calibrate the elastic stiffness of the reinforced concrete and masonry elements, for the numerical models.

The results are summarized in Table 1, which lists the natural frequencies identified for both buildings.

Specimen	Building A (no control)		Building B (with control)	
Mode	Frequency (Hz)	Direction	Frequency (Hz)	Direction
1	8.39	X	8.38	X
2	29.91	U1	31.91	U1

Table 1 – Results of experimental modal analysis.

2.3 Experimental results

For shaking intensities of up to 60% of the maximum input considered, both buildings displayed essentially elastic behavior, with Building A (un-retrofitted) experiencing some extent of cracking in the infill walls.

As the shaking intensity was increased, Building A exhibited notable diagonal cracking in the nodal panels of the first-floor slab, and in the upper part of the columns of the ground floor. In contrast, Building B (retrofitted) continued to show essentially elastic behavior, with only minor cracking of the infill walls (Figure 4) and no damage to the structural reinforced concrete elements.

The experimental program was terminated when the vertical elements of the first story of the Building A exhibited a high degree of damage, which appeared to reduce the vertical bearing capacity of the structure and its ability to absorb additional horizontal displacements.

Figure 4: Detailed view of a selected region of the Buildings: a) cracking of the column-slab joint region of the first floor in Building A, b) column-joint region of Building B with no signs of distress.

Figure 5 shows the peak first floor inter-story drifts for the two specimens during all testing phases. At shaking intensities ranging from 10% to 70% of the reference earthquake (CMP 1 to CMP 11), the maximum first story drift recorded for Building B was consistently 50% to 65% lower than that recorded for Building A.

The benefits of the AMD with respect to limiting the inter-story drift of the critical floor become even more prominent (and somewhat more relevant) in the case of high-intensity input ground motions.

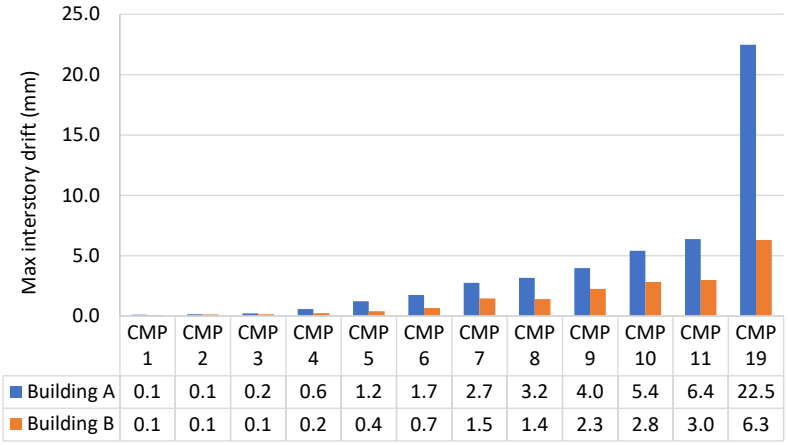

	CMP 1	CMP 2	CMP 3	CMP 4	CMP 5	CMP 6	CMP 7	CMP 8	CMP 9	CMP 10	CMP 11	CMP 19
Building A	0.1	0.1	0.2	0.6	1.2	1.7	2.7	3.2	4.0	5.4	6.4	22.5
Building B	0.1	0.1	0.1	0.2	0.4	0.7	1.5	1.4	2.3	2.8	3.0	6.3

Figure 5: Graphical and numerical representation of the maximum interstory drift recorded at the first floor of both buildings during each test.

Figure 6 illustrates the story relative (with respect to the base) displacement histories for both buildings, for two important shake intensities (CMP 8 and 19). The figure highlights the drastic reduction in displacement demand in the retrofitted specimen, Building B (-70% in CMP 19), induced by the I-Pro 1 system.

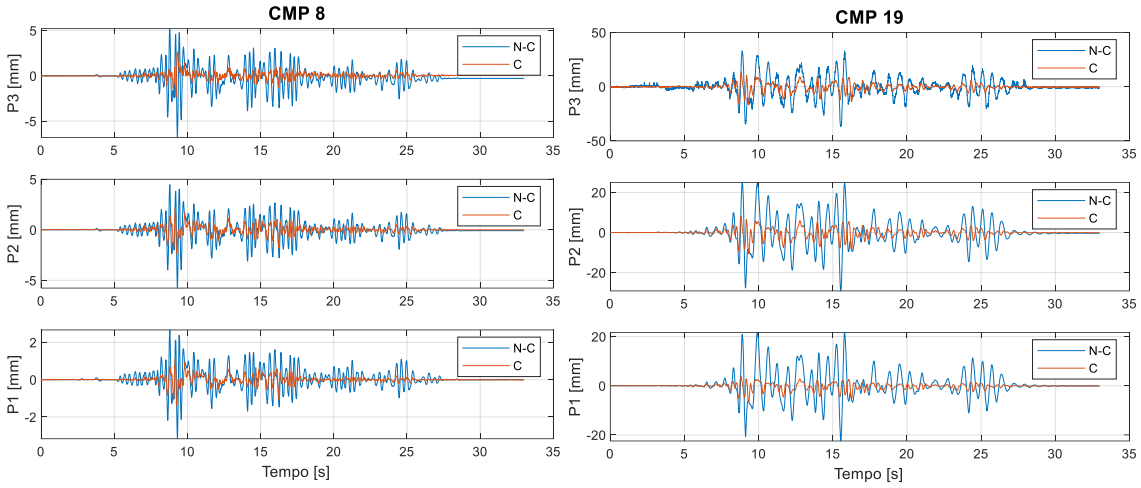

Figure 6 - Displacement histories of the floors of the Building A (N-C) and Buildings B (C).

These results demonstrate that the performance of the case study building was significantly enhanced by the presence of the AMD, in terms of inter-story drifts and overall damage to structural and non-structural elements. The two main aspects that contribute to enhancing the building seismic performance are the inertial force generated and the amount of input energy absorbed by the AMD.

3 NUMERICAL SIMULATIONS

The numerical analysis of the retrofitted (i.e. Building B) case-study structure described in the previous sections was performed using Midas Gen.

3.1 General description of the model

Several linear and non-linear FEM models of the structures were developed in order to calibrate the most important parameters governing the dynamic response of the system. All models use “beam elements” for the columns and “plate elements” with four nodes, for the floor slabs.

To simulate the non-linear behavior of the columns, a fibre-model approach based on the formulation by Spacone et al. (1996) was adopted. In particular, 10 intermediate points of integration were assigned at each “beam element” of the frame.

The concrete stress-strain response was modeled using Mander’s constitutive model (1988), considering both confined and unconfined concrete (see Table 2). The steel reinforcement was modeled using the Menegotto-Pinto approach (Mengotto & Pinto 1973), with tensile strength f_y of 450 MPa, elastic modulus E_s of 200 GPa, and hardening coefficient of 0.001.

Symbol	Quantity	Values
f_{co}’	Unconfined concrete strength	35.6 MPa
ε_{c0}	Unconfined concrete strain	0.002
f_{cc}	Strength of confined concrete	42.7 MPa
ε_{cc}	Strain for confined concrete	0.004
E_{sec}	Secant elastic modulus of concrete	10680 MPa
f_{ct}	Tensile strength of concrete	3.25 MPa

Table 2: Mander’s constitutive parameters.

The infill masonry walls were modeled as equivalent diagonal struts, in accordance with the model by Bertoldi [14]. Furthermore, to take into account the openings in the walls at ground and first floors, the formulation by Decanini [15] was used. The initial axial stiffness of the struts was calibrated to match the experimental modal response in the elastic range. Using model updating technique, the following elastic stiffness values were identified and assigned to the diagonal struts: $K_{el,PT}$ = 90 kN/mm, $K_{el,P1}$ = 115 kN/mm, $K_{el,P2}$ = 145 kN/mm (Figure 7). The struts' non-linear mechanical properties were then obtained using the model by Bertoldi, which estimates the stiffness $E_{w\Theta}$ and strength F_w of the equivalent strut as a function of the level of deformation reached (see Table 3).

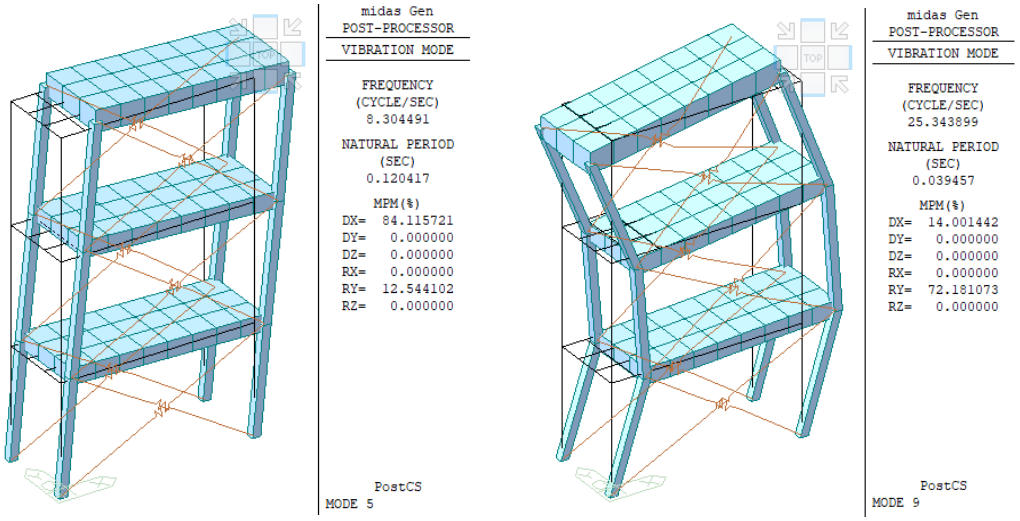

Figure 7 - First two natural modes of the building in X direction.

Symbol	Quantity	First floor	Second floor	Third floor
F_{we}	Elastic strength	57 kN	72 kN	91 kN
F_w	Peak strength	67 kN	85 kN	107 kN
$F_{w\theta}$	Post-elastic stiffness	12.2 kN/mm	15.3 kN/mm	19.4 kN/mm

Table 3: Mechanical parameters of masonry strut-link.

A residual stiffness equal to 0.1% of the elastic stiffness was considered to describe the ultimate conditions of the wall panels. This behavior was simulated by using a slip trilinear/compression-general link as shown in Figure 8.

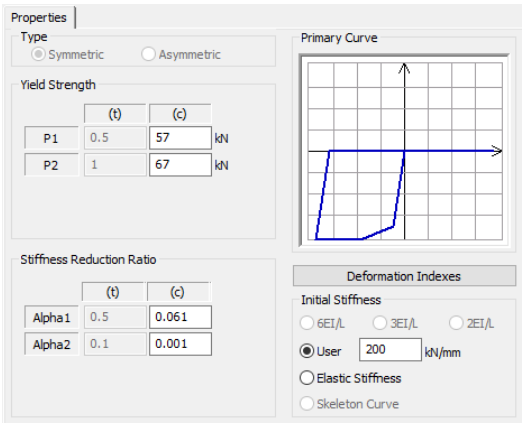

Figure 8: Plastic hinge associated with the representative link of the equivalent strut for the first floor.

The AMD is an active control system and its behavior is determined by specific algorithms and control logic. However, if some hypotheses about the mechanics of its behavior are respected in the simulation (e.g., the maximum stroke available and the maximum velocity that the mobile mass can achieve are not exceeded), the device can be approximated with a simple non-linear dashpot. This is because the control force delivered by the AMD can be computed as the product of the relative velocity of the roof of the structure (measured at the installation point) and a damping constant (see [1]). Adopting this approximation, the behavior of the AMD was simulated with four non-linear dashpots working in parallel and connected to the top level of the structure, as shown in Figure 9a. This modeling approach follows the same logic of the control algorithm of the system, hence can be identified as a "skyhook approach" modeling.

The dashpot properties are summarized in Figure 9b: each element was assigned a damping coefficient C_e = 37.5 kNs/m, providing a total coefficient of 150 kNs/m, and a relief damping force of 39.5 kN (which corresponds to 158 kN, considering the four dashpots). Beyond this limit, the force of the device becomes saturated, thus a damping coefficient near 0 was assigned to the link elements to simulate this second stage of the response.

3.2 The non-linear dynamic analysis

The case-study structure was analysed via non-linear time history, implementing the shaking sequence displayed in Fig. 3. The ground acceleration was applied in the X direction.

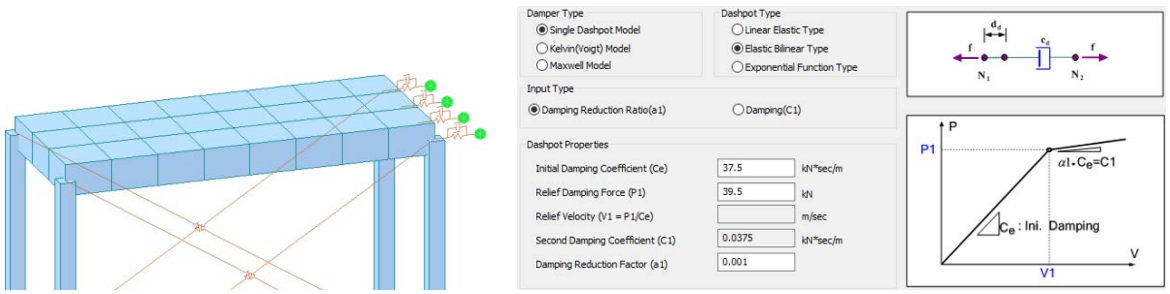

Figure 9: a) Skyhook modelling and links used to simulate the AMD; b) Setting parameters of the damper.

The Newmark's method (γ = 0.5, β = 0.25), with 256 Hz frequency integration time step, was used to solve the equation of motion. Rayleigh's formulation was chosen to define the damping of the system [16].

Figure 10 shows that the results of the numerical simulation pertaining to floor horizontal displacement, are in excellent agreement with the experimental results collected for Building B.

As depicted in Figure 11, there is also excellent agreement between the experimental AMD force and the total force in the viscous link elements used to simulate the AMD response in the numerical analysis. It worth noting that the maximum delivered force by the AMD was 50 kN, much lower than the 220 kN actuator capacity. Evidently, the actuator did not reach force-saturation during the shake-table test, and the mobile-mass kinematics respected velocity and strike length limits. Thus, the behaviour of the AMD was well represented by the dashpot model.

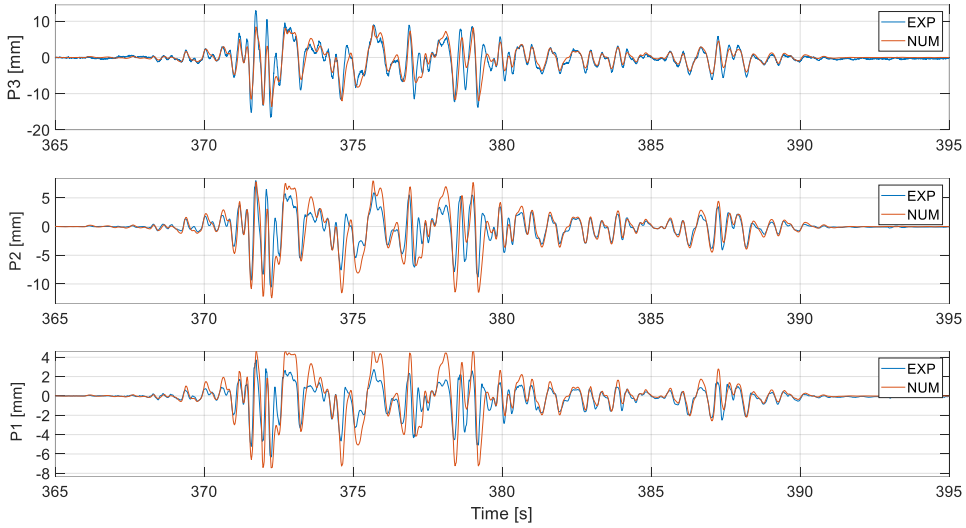

Figure 10: Experimental and numerical displacement of Building B for the last shake.

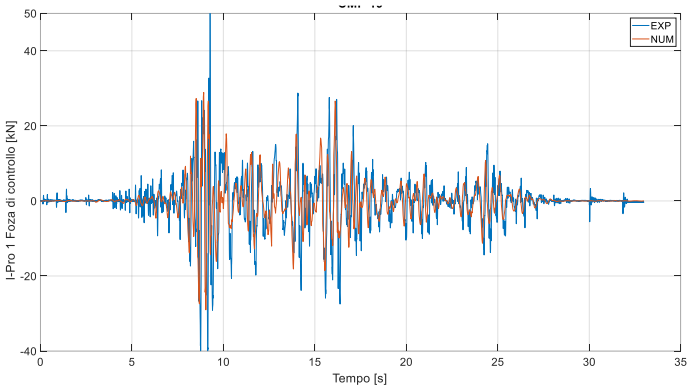

Figure 11: Comparison of the control force delivered by the AMD and the resultant force of the links in the numerical model.

4 DEVELOPMENT OF DESIGN TOOL: ISAAC-AMDesign

Although the behavior of the AMD can be modelled as a non-linear dashpot, with velocity-feedback as control algorithm, it is necessary to approach the more complex design problem using more complete calculation tools that consider the strike and velocity limits of the AMD actuator.

For this purpose, ISAAC developed “AMDesign”, a free software that implements the mechanics and control logic of the system and describes the exact movement of the mobile mass and the force delivered on the structure.

AMDesign is a plug-in app of the FEM software SAP2000 (CSi) which makes use of API (application program interface) to calculate a real-time interface between the software. The calculation loop leads to a precise simulation of the physical behavior of the building equipped with AMD system (Figure 12).

Figure 13 shows a comparison between the experimental drift of the first floor of the building measured during the last shake-table test, and the numerical drift obtained from AMDesing. It can be seen that there is excellent agreement between experimental and numerical results.

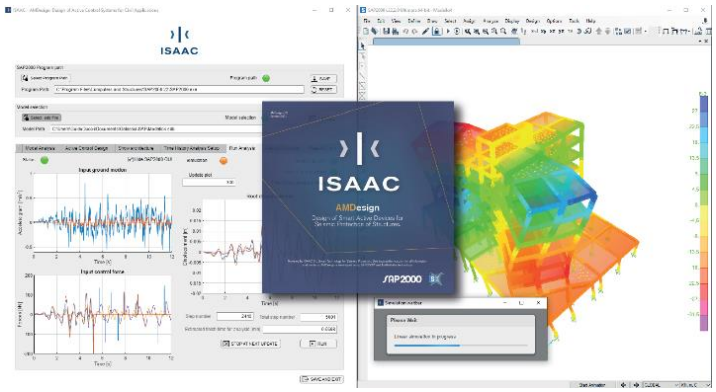

Figure 12 Screen of the free software ISAAC-AMDesign.

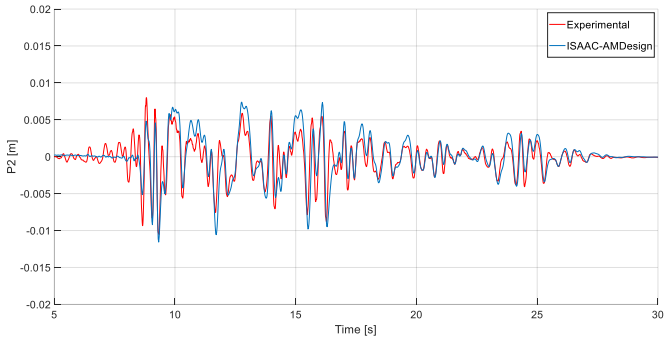

Figure 13 Comparison of the first floor drift measured during the experiment with the displacement obtained using ISAAC-AMDesign.

5 CONCLUSIONS

This paper summarized the results of an experimental program involving shake-table testing of two full-scale reinforced concrete buildings, one of which was equipped with the I-Pro 1 system. The I-Pro 1 system acts as an active mass damper, counteracting the oscillations of the substructure by exerting a control force calculated based on real-time accelerometer measurements. The results of the shake-table tests showed that, while the unretrofitted structure experienced significant damage to structural and non-structural elements, the building equipped with the novel AMD did not suffer any notable damage.

The paper also described the development of a numerical model for the retrofitted building using the FEM software Midas Gen, in which the AMD system was modeled using dashpot elements.

Finally, a design tool was introduced (AMDesign), which ISAAC developed specifically to run simulations that fully describe the operational mechanism of buildings equipped with the I-Pro 1 system. AMDesign rests on the SAP2000 software calculation core and can be used as a practical and simple tool to design the newly proposed AMD.

REFERENCES

[1] Rebecchi G., Calvi P. M., Bussini A., Dacarro F., Bolognini D., Grottoli L., Rosti M., Ripamonti F., Cii S. "Full-scale shake table tests of a reinforced concrete building equipped with a novel servo-hydraulic active mass damper", *Journal of Earthquake Engineering*, DOI: 10.1080/13632469.2022.2121338. 2022.

[2] Rosti M., Cii S., Bussini A., Ripamonti F., Calvi P.M. "Design and Validation of a Hardware-In-the-Loop Test Bench for the Performance Evaluation of an Active Mass Damper", *Journal of Vibration and Control*, under review. 2022.

[3] G De Roeck, G. D. "A versatile active mass damper for structural vibration control". 2011.

[4] Dyke S., Spencer B., Quast P., Kaspari Jr. D., Sain M. "Implementation of an active mass driver using acceleration feedback control", Microcomput. Civil Eng. 11:305–323. 1996.

[5] Forrai A., Hashimoto S., Isojima A., Funato H., Kamiyama K. "Gray box identification of flexible structures: application to robust active vibration suppression control", *Earthquake Engineering Structural Dynamics*. 30:1203–1220. 2001.

[6] Moutinho C., Cunha A., Caetano E. "Implementation of an active mass driver for increasing damping ratios of the laboratorial model of a building", *Journal of Theoretical and Applied Mechanics*. 49:791–806. 2011.

[7] S. Chu, T.Soong, A.Reinhorn, *Active Hybrid and Semi-Active Structural Control*, John Wiley and Sons, Ltd, England. 2005

[8] Saito T., Shiba K., Tamura K. "Vibration control characteristics of a hybrid mass damper system installed in tall buildings", *Earthquake Engineering Structural Dynamics*. 30:1677–1696. 2001.

[9] Xu H.B., Zhang C.W., Li H., Ou J. P. "Real-time hybrid simulation approach for performance validation of structural active control systems: a linear motor actuator based active mass driver case study", *Structural Control Health Monitoring*. 21:574–589. 2014.

[10] J. Connor, S.Laflamme, *Structural Motion Engineering*, Springer International Publishing, Switzerland, 2014.

[11] Yamamoto M., Sone T. (2014). "Behavior of active mass damper (AMD) installed in high-rise building during 2011 earthquake off pacific coast of Tohokuand verification of regenerating system of AMD based on monitoring". *Structural Control Health Monitoring*. 21:634–647.

[12] Nakamura Y., Tanaka K., Nakayama M., Fujita T. "Hybrid mass dampers using two types of electric servomotors: AC servomotors and linear-induction servomotors", *Earthquake Engineering Structural Dynamics*. 30:1719–1743. 2001.

[13] Bertero V. V., Bresler B., Selna L.G., Chopra A.K. , Koretsky A.V. "Design implications of damage observed in the Olive view medical center buildings". *Proceedings of the 5 th World Conference on Earthquake Engineering*. 1973.

[14] Bertoldi S.H., Decanini L.D., Gavarini C. – "Telai tamponati soggetti ad azioni sismiche, un modello semplificato: confronto sperimentale e numerico". *Atti del 6° Convegno Nazionale ANIDIS*, vol. 2, pp. 815– 824, Perugia, 13-15 October. 1993.

[15] Decanini L.D., Liberatore L., Mollaioli F. – "Strength and stiffness reduction factors for infilled frames with openings", *Earthquake Engineering and Engineering Vibration*, Vol. 13, No. 3, pp. 437–454. 2014.

[16] Chopra A.K. – "Dynamics of Structures", *Prentice Hall*, 2001.